

# Individualized therapy based on the combination of mini-PDX and NGS for a patient with metastatic AFP-producing and HER-2 amplified gastric cancer

XIAODAN ZHU<sup>1\*</sup>, XIAOQING XU<sup>1\*</sup>, BAONAN ZHANG<sup>1</sup>, YUN DONG<sup>2</sup>,  
SHIXIA GONG<sup>1</sup>, TINGJIE GONG<sup>1</sup>, FEIFEI ZHANG<sup>3</sup> and CHUNHUI JIN<sup>1</sup>

Departments of <sup>1</sup>Oncology and <sup>2</sup>Pathology, Wuxi Hospital Affiliated to Nanjing University of Chinese Medicine, Wuxi, Jiangsu 214071; <sup>3</sup>Shanghai LIDE Biotech, Co., Ltd., Shanghai 201203, P.R. China

Received April 7, 2022; Accepted August 23, 2022

DOI: 10.3892/ol.2022.13531

**Abstract.** Mini-patient-derived xenograft (mini-PDX) is a novel, rapid and accurate method used to assess *in vivo* drug susceptibility. In the present study, a mini-PDX combined with next-generation sequencing (NGS) was used to guide the individualized treatment of a patient with metastatic a-fetoprotein-producing and human epidermal growth factor receptor 2 (HER-2) amplified gastric cancer (GC). Tumor cells were isolated from the tumor tissue obtained from gastroscopic biopsy, transferred into capsules and implanted into severe combined immunodeficiency mice to determine their sensitivity to various drug regimens. NGS was also performed to assess the mutation spectrum of the cells. The results were analyzed to select the most appropriate treatment regimen for the patient. The mini-PDX model confirmed that the patient's tumor was sensitive to a combination regimen of irinotecan and tegafur-gimeracil-oteracil (S-1). Fluorescence *in situ* hybridization assay of the tumor tissue confirmed HER-2 amplification. The NGS results indicated ERBB2 amplification, and tumor protein P53 [c.659A>G (p.Y220C)], ataxia-telangiectasia mutated [c.125A>G (p.H42R)] and MutS homolog 6 [c.3254C(8>7) (p.F1088Sfs\*2)] mutation, in which UGT1A1\*28, TA6/7 (rs8175347) was a mutant

heterozygote. After six courses of treatment with a regimen comprising 300 mg irinotecan on day 1 + 40 mg S-1 twice daily on days 2-15 + 350 mg trastuzumab once-every 3 weeks, the patient continued with S-1 treatment for 4 courses and trastuzumab for 1 year. The patient retained progression-free survival status at the 32-month follow-up. Thus, the mini-PDX model combined with the NGS rapidly assessed drug sensitivity in a patient with GC and revealed key genetic mutations. However, the proposed technique requires further research to confirm its potential in the individualized treatment of patients with refractory malignancies.

## Introduction

Gastric cancer (GC) is a major health threat, with the highest morbidity and mortality rates among malignant tumors of the digestive system (1). GC has a strong heterogeneity in terms of biological characteristics, primary tumor sites, pathogenesis, pathological types and molecular types, which may result in varying biological behaviors and prognoses, making it challenging to treat. a-fetoprotein (AFP)-producing GC (AFPGC) is a special and rare type of GC with an incidence of 1.3-15% (2). Due to the rapid progression of AFPGC and its high rate of liver metastasis, some patients with AFPGC are inoperable at the time of diagnosis. Furthermore, those who undergo radical surgical resection are more likely to experience postoperative recurrence and metastasis, and chemotherapy is less effective for AFPGC than for gastric adenocarcinoma (3).

The standard first-line treatment for advanced or recurrent GC is chemotherapy combined with immunotherapy. For cases with human epidermal growth factor receptor-2 (HER-2) amplification, the use of trastuzumab in combination with a molecular targeted drug is recommended. The chemotherapy regimen is commonly a combination of two or three fluorouracil- and platinum-based drugs (4,5). The second- and third-line treatments mainly include single-drug therapies with a low efficacy. At present, there is no universal standard treatment regimen. As a result, the selection of drugs may be quite random. Although an experimental treatment plan can be applied, it may delay the treatment process and thus worsen the patients' quality of life. There is currently no efficient method

*Correspondence to:* Dr Chunhui Jin, Department of Oncology, Wuxi Hospital Affiliated to Nanjing University of Chinese Medicine, 8 Zhongnan West Road, Wuxi, Jiangsu 214071, P.R. China  
E-mail: wxzy013@njucm.edu.cn

\*Contributed equally

**Abbreviations:** PDX, patient-derived xenograft; NGS, next-generation sequencing; AFPGC, a-fetoprotein-producing gastric cancer; HAS, hepatoid adenocarcinoma of the stomach; S-1, tegafur-gimeracil-oteracil

**Key words:** a-fetoprotein-producing gastric adenocarcinoma, HER-2 amplification, mini patient-derived xenograft, next-generation sequencing, personalized therapy

for the assessment of a cancer patient's sensitivity to chemotherapeutic drugs. Therefore, the accurate selection of medical treatment, particularly mediated via effective drug-screening models, is urgently necessary to improve adjuvant treatment or second-line therapy.

Patient-derived xenografts (PDXs) can be used for the pre-evaluation of therapeutic outcomes (6). In contrast to cell line-derived tumor models, PDX models retain the genetic characteristics of the human tumor specimens from which they were derived (7). PDX models are generated by the implantation of fresh human tumor tissues into immunodeficient mice, to reduce rejection of the tumor cells by the mouse. PDX models can effectively simulate the treatment response of the parent tumors and provide information that may aid the selection of therapeutic targets and protocols (8,9). To date, the application of traditional PDX models in individualized treatment has failed due to the low success rate and lengthy implantation period of the models. PDX modeling is also expensive, technically cumbersome and requires a large amount of tumor tissue (10). Mini-PDX is a drug sensitivity test model that maintains the oncogenicity of a patients' tumor cells, in which cells from human tumor tissues are injected into immunocompromised mice within special capsules to create tumor xenografts; this is a promising model accompanied by reduced complexity and faster turnaround compared with traditional PDX models.

The present study aimed to evaluate the application of the mini-PDX model combined with genetic analysis of tissue samples to guide the individualized treatment of a patient with metastatic AFGC and HER-2-positive GC.

## Materials and methods

**Patient and ethics.** A 74-year-old male patient with gastric cancer was included in the study. The patient underwent gastroscopy at Wuxi Hospital Affiliated to Nanjing University of Chinese Medicine (Wuxi, China) on December 17, 2018. The study protocol was approved by the Institutional Review Board of Wuxi Hospital of Traditional Chinese Medicine (approval no. 201809001J01-01) and the Institutional Animal Care and Use Committee (IACUC) of Shanghai LIDE Biotech Co., Ltd. (approval no. LDIACUC007).

**Histopathological examination.** A portion of the tumor tissue was detached and fixed by immersion in 10% neutral buffered formalin solution (pH 7.4) for 12 h at 24°C. The portion was then cut transversely, paraffin embedded and arranged as 3- $\mu$ m sections, which were stained with hematoxylin and eosin (H&E) for 20 min at 24°C for the microscopic assessment of tumor tissue. The tissues were examined under a light microscope in a random order.

**Immunohistochemistry.** Tumor tissues were fixed with 4% paraformaldehyde for 24 h at 24°C, and the fixed tissues were dehydrated and embedded in paraffin. Later, 4- $\mu$ m sections of the paraffin-embedded tissues were prepared. Endogenous peroxidase activity was blocked by incubating the tissues at 25°C with 0.6% H<sub>2</sub>O<sub>2</sub> in methanol for 20 min. Sections were subsequently blocked with 10% normal horse serum (Wuhan Boster Biological Technology, Ltd.) for 5 min at 25°C. Next,

the sections were incubated at 4°C overnight with AFP antibody (1:50; cat. no. ab130748; Abcam). The slides were then incubated with the secondary antibody Goat Anti-Rabbit IgG (1:2,000; cat. no. ab205718; Abcam) for 30 min at room temperature. Subsequently, DAB chromogen (cat. no. ab64238; Abcam) was added to the tissue and incubated for 1-10 min, depending on the desired stain intensity. The sections were rinsed four times in PBS and were subsequently stained with hematoxylin and hydrochloric acid alcohol for 20 min at 24°C, followed by washing with tap water for 10 min. After dehydration and transparency, the tissue sections were analyzed under a bright-field Olympus BX-40 light microscope (Olympus Corporation). The classification of nuclear AFP expression was assessed using the following scores: Unstained, 0; <25% positive cells, 1+; 25-50% positive cells, 2+; 50-75% positive cells, 3+; and >75% positive cells, 4+.

**Fluorescence in situ hybridization (FISH).** A PathVysion HER-2 DNA probe kit was purchased from Vysis Inc. (Abbott Molecular, Inc.). A fluorescence microscope (Bx51; Olympus Corporation) was used to view the FISH staining. The HER-2/neu gene FISH test was performed on the tumor tissue according to the instructions and requirements of the kit.

**Mini-PDX assay.** A Mini-PDX assay was carried out using the OncoVee MiniPDX<sup>®</sup> kit (LIDE Biotech Co., Ltd.) in the joint animal laboratory of Wuxi Hospital and Shanghai LIDE Biotech Co., Ltd. under the guidance of a researcher from LIDE. Briefly, the tumor from the patient's gastroesophageal junction was harvested and washed with Hanks' balanced salt solution (HBSS) to remove non-tumor and necrotic tumor tissue. The tumor tissues were minced and incubated with collagenase at 37°C for 1-2 h. After this, the tumor cells were incubated with human anti-CD45 microbeads (cat. no. 130-045-80, Miltenyi Biotec, Inc.) and human anti-fibroblast microbeads (cat. no. 130-050-601; Miltenyi Biotec, Inc.) at 4°C for 30 min in the dark, at a final fixed volume of 220  $\mu$ l, including 20  $\mu$ l beads, 10<sup>6</sup> cells and buffer (PBS and 1% FBS). Subsequently, tumor cell suspensions without blood cells or fibroblasts were eluted with 1 ml buffer and collected. The remaining cell suspension was transferred to HBSS-washed capsules made of hollow fiber membranes with a pore size allowing the passage of <500-kDa molecules; eventually each capsule contained 2,000 cells. A fiber system delivered media to the cells in a manner similar to the delivery of blood through capillary networks *in vivo*. A total of 8 female severe combined immunodeficiency mice (6-8 weeks old) with average weight of ~24 g (range, 22-28 g) were housed and monitored under specific-pathogen-free conditions. The housing conditions comprised a temperature of 20-26°C, humidity of 40-70% and a 12-h light/dark cycle (11). Throughout the experiment, all mice were able to eat and drink freely; feed and water were autoclaved and replaced twice a week. For subcutaneous implantation, the capsule was inserted through the subcutaneous tissue via a special needle without any anesthesia being necessary. One day after implantation of the tumor cell-containing capsule, the tumor-bearing mice were randomized to the following groups: Vehicle; docetaxel + S-1; capecitabine + oxaliplatin; and irinotecan + S-1. S-1 is tegafur-gimeracil-oteracil, also known as tegio. The treatment regimens were as follows: 20 mg/kg docetaxel

intraperitoneally (ip) every fourth day x2 (Q4D\*2) + 10 mg/kg S-1 ip every day for 5 days (QD\*5); 400 mg/kg capecitabine orally (po) every day for 7 days + 5 mg/kg oxaliplatin ip once weekly; and 50 mg/kg irinotecan ip Q4D\*2 + 5 mg/kg S-1 po QD\*5 (12). Each mouse received 6 capsules at the same time and each regimen was tested in two mice. The final results were calculated as the average of six repeated trials. The relative change in body weight (RCBW) was calculated each day as follows:  $RCBW = (BW_i - BW_0) / BW_0 \times 100\%$ , where  $BW_i$  is the average weight on day  $i$  during drug administration and  $BW_0$  is the average weight at the first administration. After 7 days, the tumor cell-containing capsules were removed. After the experiment, the mice were euthanized via CO<sub>2</sub> inhalation in a euthanasia chamber (50% chamber replacement rate/min) followed by cervical dislocation, or by the administration of 0.1% ketamine sodium (100 mg/kg, intraperitoneal injection) (13) followed by cervical dislocation.

The viability of the cells was evaluated using a CellTiter-Glo<sup>®</sup> Luminescent Cell Viability Assay kit (G7571; Promega Corporation), following the manufacture's protocol. The tumor cell proliferation rate relative to that of the control group after the 7-day treatment was calculated using the following equation: Relative proliferation rate =  $T/C \times 100\%$ , where  $T$  and  $C$  are the cell viability values for the treatment and control group, respectively. A lower relative proliferation rate indicated a higher inhibitory effect of the drugs on the tumor cells.

**Next-generation sequencing (NGS).** DNA was extracted from formalin-fixed, paraffin-embedded (FFPE) tumor tissue samples using the QIAamp DNA FFPE Tissue kit (Qiagen GmbH). In addition, 3 ml peripheral blood from the patient was collected in an EDTA Vacutainer tube (BD Diagnostics) and processed within 4 h. Peripheral blood lymphocytes (PBLs) were separated by centrifugation at  $1,600 \times g$  for 10 min at room temperature and used for the extraction of germline genomic DNA, which served as the reference for germline variation and single nucleotide polymorphism identification. The DNA concentration in the PBLs and tissues was measured using a Qubit<sup>™</sup> Flex kit and the Qubit DNA Assay kit (both Invitrogen; Thermo Fisher Scientific, Inc.). DNA sequencing was carried out using 2x75-bp scanned-end reads on an Illumina HiSeq 3000 system (Illumina, Inc.) and the KAPA DNA Library Preparation kit (cat. no. KK8234; Kapa Biosystems; Roche Diagnostics); the loading concentration was 40.02 ng/ $\mu$ l. DNA sequencing was applied to a panel of 73 cancer-related genes in gastric adenocarcinoma. Targeted gene sequencing was performed in the tumor and paired PBLs with an average sequencing depth of 3850X and 431X, respectively. More than 99% of the readings were mapped to areas where the tumor and matched PBL samples were targeted. Sequencing data were analyzed using software at default parameters. Adaptor sequences and low-quality reads were removed. The clean reads were aligned to the reference human genome (hg19) using Burrows-Wheeler Aligner (version 0.7.12-r1039) (14). Realignment and recalibration were performed using Genome Analysis Toolkit (version 3.4-46-gbc02625) (15). Single nucleotide variants were called using MuTect (version 1.1.4) (16).

**Statistical analysis of mini-PDX.** Statistical analyses were performed using SPSS version 22.0 (IBM Corp.). One-way ANOVA followed by Tukey's post hoc test was used for evaluating differences among groups.  $P < 0.05$  was considered to indicate a statistically significant difference.

## Results

**Clinical data.** The 74-year-old male patient presented with a bloated and uncomfortable upper abdomen and underwent gastroscopy on December 17, 2018. Gastroscopy revealed a large ulcer from the cardia to the fundus of the stomach. The pathology examination confirmed adenocarcinoma. Abdominal contrast-enhanced computed tomography (CT) revealed a mass in the lesser curvature of the stomach. Combined with the medical history, the mass was initially considered as a swollen lymph node. The gastric wall was thickened in the cardiac part, gastric fundus and lesser curvature of the stomach. Bronchiectasis with infection was detected in the right lung. Considering that the patient had a history of bronchiectasis for >10 years, his extremely poor pulmonary function indicated that he was an inappropriate candidate for GC surgery. A serum test performed in January 2019 revealed an AFP level of >1,210 ng/ml, while the levels of carcinoembryonic antigen, carbohydrate antigen 19-9 and carbohydrate antigen 72-4 were all within the normal range. Gastroscopy showed the presence of carcinoma of the lower esophagus near the cardia, which the endoscope could not pass (Fig. 1A) due to obstruction of the lumen. At the same time, tumor tissue was biopsied for the mini-PDX assay. Pathology confirmed adenocarcinoma (Fig. 2). Immunohistochemical assay showed the following results: HER-2 (2+), epidermal growth factor receptor (EGFR)+ (weak), Ki-67+ (~50%), P53+ (diffuse) and AFP-. The FISH assay indicated HER-2 amplification (Fig. 3). Contrast-enhanced CT examination of the upper abdomen revealed swollen lymph nodes with a size of ~4.5x3.5 cm in the lesser curvature of the stomach (Fig. 4A).

**Mini-PDX assay.** In this assay, after 7 days of drug treatment, the mini-PDX devices were removed from the mice and the relative proliferation rates of the tumor cells were determined. The results revealed that tumor cell proliferation in the three treatment groups [irinotecan + S-1 (tumor (T)/control (C)=16%), docetaxel + S-1 (T/C=29%) and capecitabine + oxaliplatin (T/C=40%)] was significantly lower than that in the control group, demonstrating the strong inhibitory effect of the three regimens on the growth of tumor cells. The irinotecan + S-1 group had the lowest relative tumor cell proliferation rate, which indicated that this regimen had the strongest inhibitory effect (Fig. 5A). Furthermore, no significant reduction in body weight of mice was observed in any group during the experiment, which suggested that the dosage of the drug regimen was within the safe range (Fig. 5B).

**NGS.** The following somatic genetic changes were detected in the primary tumor: Tumor protein P53 [c.659A>G (p.Y220C); 52.6%], ataxia-telangiectasia mutated [ATM; c.125A>G (p.H42R); 48.1%] and MutS homolog 6 [c.3254C(8>7) (p.F1088Sfs\*2); 5.4%] mutation, and ERBB2 (HER-2) amplification. In addition, the following genomic biomarkers



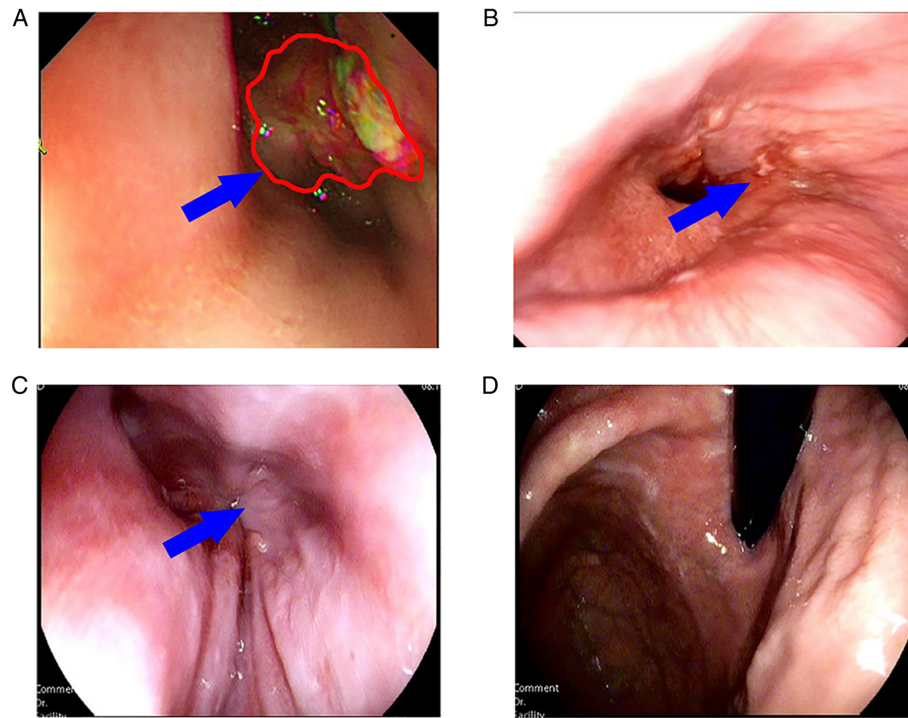


Figure 1. Gastroscopic images of the patient in which the blue arrow indicates the tumor focus and the red outline represents the tumor focal boundary. (A) On January 11, 2019, a tumor lesion at the gastroesophageal junction blocked the esophageal lumen, preventing endoscopic exploration. (B) On May 22, 2019, the tumor was largely diminished and the endoscope was able to pass through the cardia. (C) Cardia and (D) fundus of the stomach were examined by gastroscopy on May 17, 2021, and no tumor tissue was visible with the naked eye.

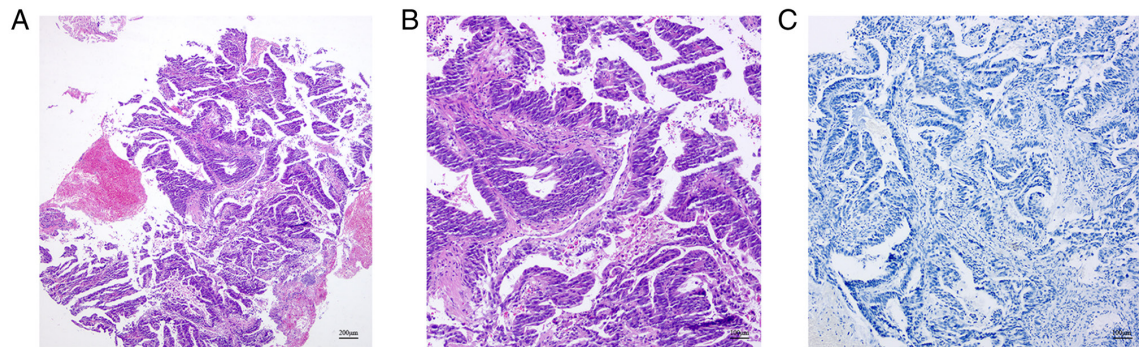


Figure 2. Histopathological examination of adenocarcinoma of the esophagogastric junction. (A and B) Hematoxylin and eosin staining reveals abnormal glands with villous hyperplasia, massive necrosis and no hepatolenticular differentiation. (A) magnification x40; (B), magnification x100. (C) Immunohistochemical analysis of  $\alpha$ -fetoprotein did not detect any expression; magnification, x100.

associated with chemotherapeutic drugs were detected: Capecitabine and fluoropyrimidines [dihydropyrimidine dehydrogenase (DPYD) rs3918290 (DPYD\*2A), DPYD rs55886062 (DPYD 1679 T>G) and DPYD rs67376798 (DPYD 2846 A>T)] and irinotecan [UDP glucuronosyltransferase family member 1 A1 (UGT1A1) rs8175347 (UGT1A1\*28, TA6/7) and UGT1A1 rs4148323 (UGT1A1\*6, GG)], which indicates that these drugs had a low risk of side effects.

**Chemotherapy.** The results of the mini-PDX assay indicated that the irinotecan + S-1 treatment regimen had the strongest inhibitory effect on the tumor cells, and the results of NGS indicated that capecitabine, fluoropyrimidines and irinotecan had a low risk of side effects. The combination of the results from both assays suggested that irinotecan +

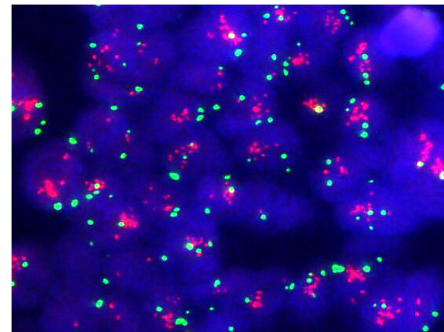


Figure 3. Fluorescence *in situ* hybridization assay. Fluorescence microscopy shows HER-2 in red and CEP17 in green, with a HER-2/CEP17 ratio of 3.64 ( $\geq 2$ ) and average copy number of HER-2 of 8.32 ( $\geq 6$ ), indicating HER-2-positivity, magnification, x100. HER-2, human epidermal growth factor receptor 2; CEP17, chromosome 17 centromere.

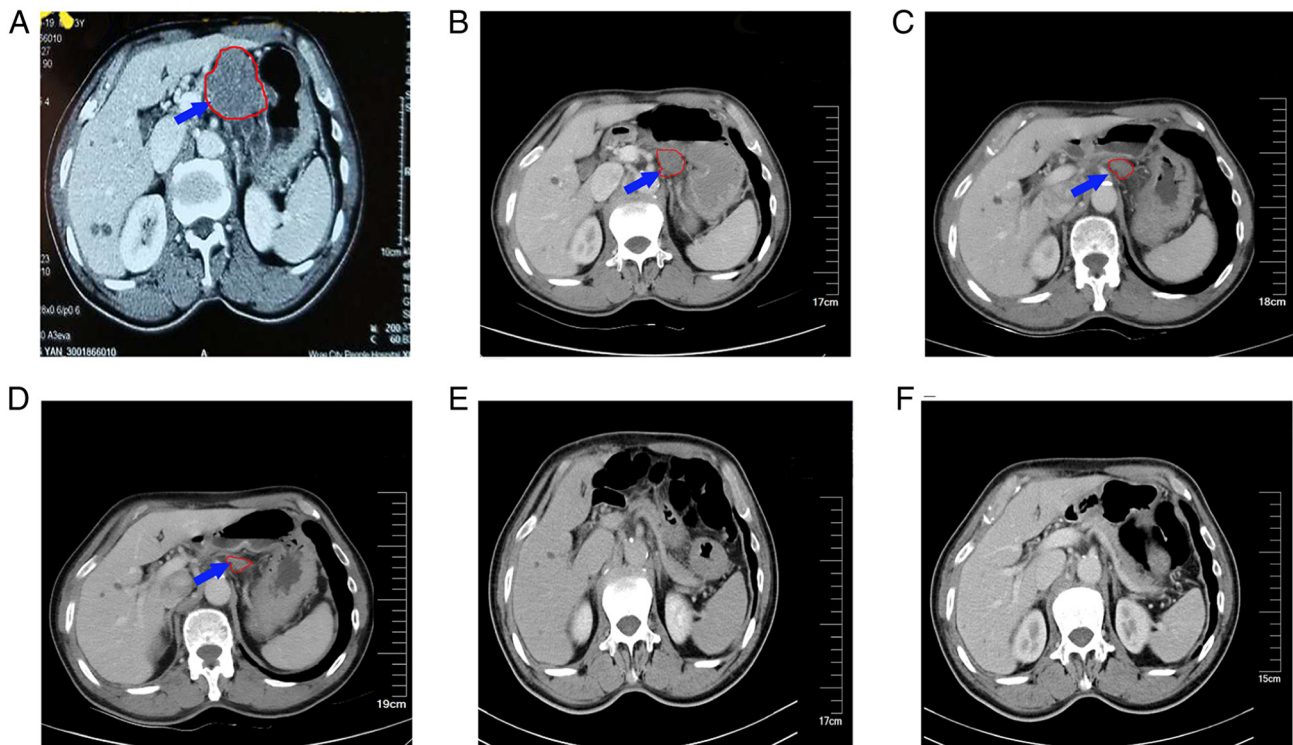


Figure 4. Abdominal enhanced CT in which the blue arrow and red outline indicate swollen lymph nodes and their boundary at the lesser curvature of stomach, which gradually shrank and then disappeared after treatment. (A) Abdominal CT scan performed on December 17, 2018, showing lymph nodes in the lesser curvature of the stomach ~4.5x3.5 cm in size. (B) Abdominal CT scan carried out on March 7, 2019, showing that the lymph nodes in the lesser curvature of the stomach had decreased to ~3.5x2.5 cm. (C) Abdominal CT scan performed on May 23, 2019, showing a further reduction in the size of the lymph nodes to ~2.5x1.5 cm. (D) Abdominal CT carried out on October 21, 2019, indicating that the size of the lymph nodes was ~2x1.1 cm. Abdominal contrast-enhanced CT scans performed on (E) August 18, 2020 and (F) May 11, 2021, showing that the enlarged lymph nodes in the lesser curvature had disappeared. CT, computed tomography.

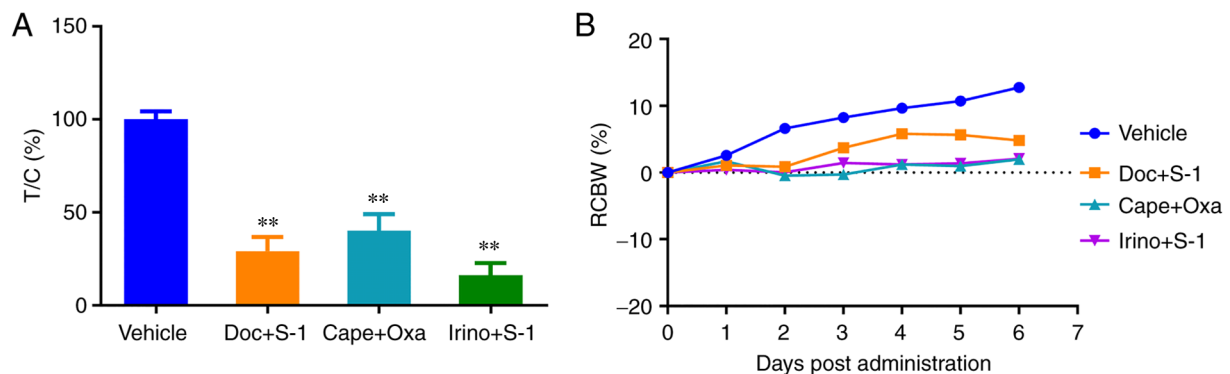


Figure 5. Response of the mini-PDX to various chemotherapy regimens and the change of body weight during drug delivery. (A) The proliferation of tumor cells in mini-PDX implants was observed in mice treated with vehicle, Doc + S-1, Cape + Oxa and Irino + S-1. The drug treatment began 1 day after tumor cell implantation. The tumor cell proliferation rate relative to that of the control group was calculated after the 7-day treatment. \*\*P<0.001 vs. the vehicle group. (B) The change in body weight of the mice was monitored. Throughout the experiment, no significant reduction in the weight of mice in each group was detected, suggesting that the dosage of the drug regimen was within the safe range. T, tumor; C, control; Doc, docetaxel; Cape, capecitabine; Oxa, oxaliplatin; Irino, irinotecan; S-1, tegafur-gimeracil-oteracil (tegio); RCBW, relative change in body weight.

S-1 was an appropriate regimen for chemotherapy in this patient.

Patients with concurrent HER-2 amplification can be treated with a combination of trastuzumab and targeted therapy. Considering the patient's advanced age, poor pulmonary function and lymph node metastasis in the lesser curvature of the stomach, the patient and his family requested medical treatment and refused surgery. From January 22,

2019, the treatment plan comprising a regimen of 300 mg irinotecan (day 1) plus 40 mg S-1 (twice daily, days 2-15) plus 350 mg trastuzumab (once every 3 weeks) was initiated. After the second course of treatment, the patient's AFP level was reduced to 22.78 ng/ml, which was maintained within the normal range thereafter (Fig. 6). Following two courses of treatment, gastroscopy showed that the size of the lesion was significantly reduced, allowing the endoscope to pass

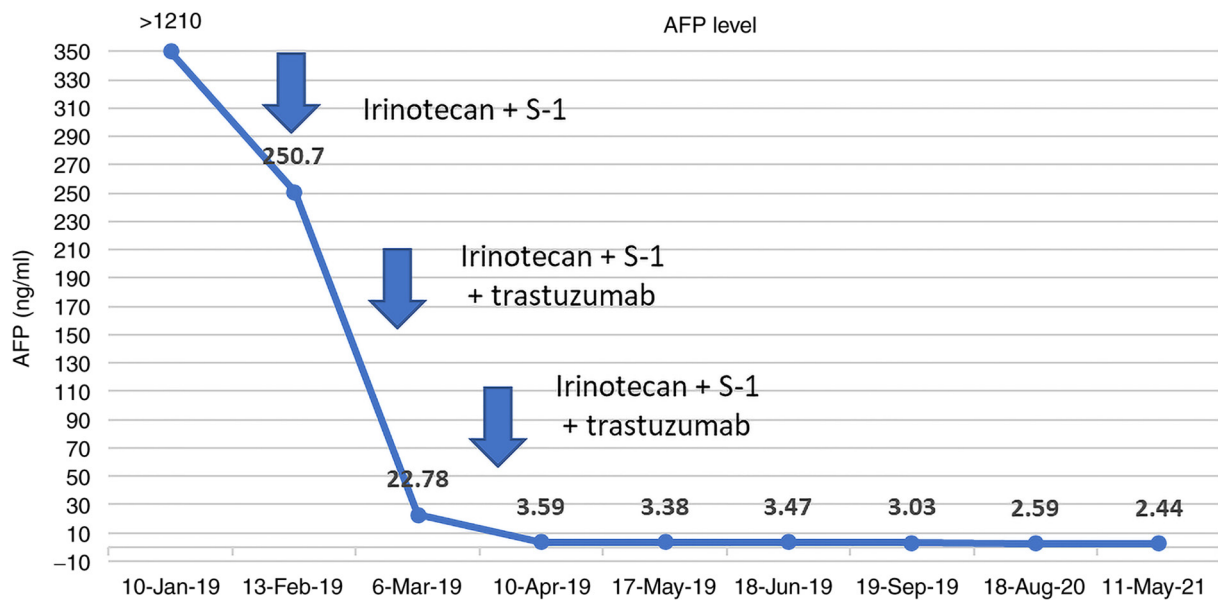


Figure 6. Changes in the AFP level of the patient. Chemotherapy was administered with a regime of 300 mg irinotecan (day 1) plus 40 mg S-1 twice daily (days 2-15) plus 350 mg trastuzumab once every 3 weeks starting on January 22, 2019. After the second course of treatment, the AFP level had fallen to 22.78 ng/ml and was within the normal range. AFP, a-fetoprotein; tegio, tegafur-gimeracil-oteracil (S-1).

through the stenosis. In addition, the lymph nodes of the lesser curvature of the stomach gradually decreased in size and then disappeared (Figs. 1B and 4B-D). After six courses of chemotherapy, the patient continued to take four courses of S-1 capsules and trastuzumab for a year. Afterwards, the drug was discontinued and the patient was followed up regularly. In May 2021, gastroscopy did not show any tumor (Fig. 1C and D) and there was no sign of recurrence or metastasis (Fig. 4E and F). To date, the patient has been experiencing a high quality of life.

## Discussion

GC is a common malignancy. A large number of patients with GC are diagnosed in the middle- or late-stage, and AFP GC is associated with a poorer prognosis than other types of GC (17). AFP GC is reported to comprise two types, one of which is hepatoid adenocarcinoma of the stomach (HAS), a rare aggressive tumor with hepatocellular differentiation (18,19). The differentiation of HAS is an important feature, particularly in hepatic lymph node metastasis (20). However, the positive rate of AFP in patients with HAS is 54-87%, indicating that AFP is not present in all HAS cases (18,19). The other type of AFP GC is the embryonic gastrointestinal type, which constitutes 11.1-26.7% of all cases of AFP GC. The intestinal mucosa of this type can mimic embryonic intestinal mucosa and produce AFP (21). Regardless of the type, serum AFP-positive GC is more malignant than other types of GC, and more prone to hepatic lymph node metastasis. Pathological stage, serum AFP level, age and hepatic metastasis are independent risk factors for the prognosis of AFP GC (22). Therefore, there is an urgent requirement for *in vivo* human models of AFP GC to determine the sensitivity of drugs used for the personalized treatment of cancer patients.

The PDX model can accurately reflect patients' sensitivity to drugs in certain types of cancer (23). However, the

limitations of the PDX model inhibit its broad application in clinical practice: Firstly, the PDX model has a low success rate and requires a large quantity of tumor tissue, which can only be obtained from surgically removed tumors; secondly, PDX modeling requires 4-8 months to determine the efficacy of treatment for a specific cancer, and the time lag between the transplantation of tumor tissue into mice and the initiation of treatment limits its extensive application (7,24). To overcome these limitations, the mini-PDX model has emerged to assist clinicians in the selection of chemotherapeutic agents. The mini-PDX model requires only a small number of tumor cells and rapidly analyzes drug sensitivity in an average testing time of 7 days, enabling patients to receive individualized chemotherapy over a clinically relevant time frame. A previous study showed a strong consistency between mini-PDX- and PDX-based drug sensitivity predictions for a variety of solid tumors, including lung cancer, pancreatic cancer and stomach cancer, with an overall response consistency of 89%, indicating that the mini-PDX-based drug sensitivity model can be used to predict the outcome of patients with cancer (12).

Patients with unresectable AFP GC are recommended to be treated with chemotherapy. In a previous study on patients with HAS receiving the same chemotherapy regimen, it was shown that the disease-free and disease-specific survival rates of patients receiving neoadjuvant chemotherapy were significantly higher than those undergoing postoperative chemotherapy (25). Therefore, neoadjuvant chemotherapy is recommended for patients with liver and/or distant metastases at the initial diagnosis. Several chemotherapeutic regimens, including cisplatin combined with fluorouracil and epirubicin, or irinotecan combined with mitomycin, have been reported to effectively slowdown the progression of AFP GC (26). In the present study, using the mini-PDX model, it was identified that irinotecan combined with S-1 had the strongest antitumor effect among the regimens tested, and NGS suggested that irinotecan would be less toxic. Satisfactory outcomes and



complete remission (CR) were achieved using the combination of irinotecan and S-1 with trastuzumab, and no third-degree or more toxic side effects were observed. The patient had HER-2 amplification, as confirmed by the FISH and NGS results. A previous study showed that the positive rate of HER-2 in patients with HAS was 42.68%, which was higher than that in patients with other types of GC (27). However, a review of studies on AFPGC suggested that when compared with GC with a normal AFP level, vascular endothelial growth factor is upregulated in AFPGC while the HER-2 expression level is not significantly different (28). In GC, the interaction between hepatocyte growth factor and its receptor c-Met can promote mitosis and cell migration, which promotes tumor development. A previous study demonstrated that the positive rate of c-Met in patients with AFPGC was higher than that in patients with AFP-negative GC. Moreover, it revealed that the difference in c-Met expression levels between the AFP (+) cells and AFP (-) cells in AFPGC tissues was not statistically significant (29). In the present study, the NGS of the tumor tissue did not suggest c-Met amplification. Instead, the patient was revealed to have HER-2 amplification, and promising results were obtained using trastuzumab. A previous study on the treatment of patients with GC of different HER-2 statuses revealed that HER-2-positive patients treated with trastuzumab had a median overall survival of 22.3 months (30). At the time of writing, the present case had survived for more than 32 months with CR, which has rarely been reported. Since immunotherapy has not been validated as a first-line treatment for patients with advanced GC, no immunohistochemistry of programmed death-ligand 1 was performed in the present case, and no programmed cell death protein 1 (PD-1) inhibitor was administered. However, if the condition progresses again, according to the KEYNOTE-811 clinical trial (31), PD-1 inhibitors may also be included in the therapeutic scheme. In addition, the NGS results identified the presence of ATM mutations. ATM is a tumor suppressor gene (32). It interacts with numerous proteins that co-localize at sites of DNA damage, where it plays an important role in genome stability and the repair of DNA damage. Therefore, its mutation may lead to homologous recombination repair deficiency. However, PARP inhibitors can comprehensively kill tumor cells with homologous recombination defects (33). Notably, patients who initially respond to PARP inhibitors may later develop resistance.

In conclusion, the present study supports the use of a mini-PDX model in combination with the NGS to optimize the clinical management of metastatic gastric adenocarcinoma.

### Acknowledgements

The authors would like to thank to Dr Yuange He (Geneplus-Beijing Institute, Beijing, China) and Dr Zhenle Bi from (Shanghai LIDE Biotech, Co., Ltd., Shanghai, China) for their technological support.

### Funding

The study was financially supported by the Precision Medicine Special Project of Wuxi Municipal Health Commission (grant no. J2011801).

### Availability of data and materials

The datasets used and/or analyzed during the current study are available from the corresponding author on reasonable request.

### Authors' contributions

CJ and XZ were responsible for the conception and design of the study. CJ provided administrative support. XX, YD, SG and TG performed clinical study and analyzed clinical data. XX and BZ analyzed and interpreted the data. FZ performed the Mini-PDX experiment. All authors contributed to writing the manuscript. All authors read and approved the final version of the manuscript. CJ and XZ confirm the authenticity of all the raw data.

### Ethics approval and consent to participate

This study was performed in accordance with the Declaration of Helsinki. The study protocol was approved by the Institutional Review Board of Wuxi Hospital of Traditional Chinese Medicine (approval no. 201809001J01-01) and the Institutional Animal Care and Use Committee (IACUC) of Shanghai LIDE Biotech Co., Ltd. (approval no. LDIACUC007). Written informed consent was obtained from the patient prior to enrollment.

### Patient consent for publication

The patient provided consent for publication of the data.

### Competing interests

FZ is an employee of Shanghai LIDE Biotech, Co., Ltd., who manufactured the miniPDX kit used for the animal experiments. The other authors declare that they have no competing interests.

### References

1. International Agency for Research on Cancer (IARC): World Cancer Day: Breast overcancer takes lung cancer as leading cause of worldwide cancer. IARC showcases key research projects to address breast cancer. IARC, Lyon, 2021. [https://www.iarc.who.int/wp-content/uploads/2021/02/pr294\\_e.pdf](https://www.iarc.who.int/wp-content/uploads/2021/02/pr294_e.pdf). Accessed February 4, 2021.
2. Yang J, Wang R, Zhang W, Zhuang W, Wang M and Tang C: Clinicopathological and prognostic characteristics of hepatoid adenocarcinoma of the stomach. *Gastroenterol Res Pract* 2014; 140587, 2014.
3. Wang YK and Zhang XT: AFP-producing gastric cancer and hepatoid gastric cancer. *Zhonghua Zhong Liu Za Zhi* 39: 801-807, 2017 (In Chinese).
4. Jang Y, Peng Z, Wei B, *et al*: Lymph node metastasis of early submucosal gastric cancer: A report of 290 cases. *World Chin J Dig* 19: 2970-2973, 2011.
5. Wang J, Tian SD and Chen XY: Advances in the treatment of advanced gastric cancer. *Chin Clin Oncol* 37: 171-175, 2010 (In Chinese).
6. Aparicio S, Hidalgo M and Kung AL: Examining the utility of patient-derived xenograft mouse models. *Nat Rev Cancer* 15: 311-316, 2015.
7. Hidalgo M, Amant F, Biankin AV, Budinská E, Byrne AT, Caldas C, Clarke RB, de Jong S, Jonkers J, Mælandsmo GM, *et al*: Patient-derived xenograft models: An emerging platform for translational cancer research. *Cancer Discov* 4: 998-1013, 2014.

8. Izumchenko E, Meir J, Bedi A, Wysocki PT, Hoque MO and Sidransky D: Patient-derived xenografts as tools in pharmaceutical development. *Clin Pharmacol Ther* 99: 612-621, 2016.
9. Zhang L, Nomi K, Zhang H, Bell T, Pham L, Kadri S, Segal J, Li S, Zhou S, Santos D, *et al*: B-cell lymphoma patient-derived xenograft models enable drug discovery and are a platform for personalized therapy. *Clin Cancer Res* 23: 4212-4223, 2017.
10. Byrne AT, Alf  rez DG, Amant F, Annibali D, Arribas J, Biankin AV, Bruna A, Budinsk   E, Caldas C, Chang DK, *et al*: Interrogating open issues in cancer precision medicine with patient-derived xenografts. *Nat Rev Cancer* 17: 254-268, 2017.
11. Xian Y, Xie Y, Song B, Ou Z, Ouyang S, Xie Y, Yang Y, Xiong Z, Li H and Sun X: The safety and effectiveness of genetically corrected iPSCs derived from  $\beta$ -thalassaemia patients in nonmyeloablative  $\beta$ -thalassaemic mice. *Stem Cell Res Ther* 11: 288, 2020.
12. Zhang F, Wang W, Long Y, Liu H, Cheng J, Guo L, Li R, Meng C, Yu S, Zhao Q, *et al*: Characterization of drug responses of mini patient-derived xenografts in mice for predicting cancer patient clinical therapeutic response. *Cancer Commun (Lond)* 38: 60, 2018.
13. Overmyer KA, Thonusin C, Qi NR, Burant CF and Evans CR: Impact of anesthesia and euthanasia on metabolomics of mammalian tissues: Studies in a C57BL/6J mouse model. *PLoS One* 10: e0117232, 2015.
14. Li H and Durbin R: Fast and accurate short read alignment with Burrows-Wheeler transform. *Bioinformatics* 25: 1754-1760, 2009.
15. Aaron MK, Matthew H, Eric B, Sivachenko A, Cibulskis K, Kernysky A, Garimella K, Altshuler D, Gabriel S, Daly M and DePristo MA: The genome analysis toolkit: A MapReduce framework for analyzing next-generation DNA sequencing data. *Genome Res* 20: 1297-1303, 2010.
16. Cibulskis K, Lawrence MS, Carter SL, Sivachenko A, Jaffe D, Sougnez C, Gabriel S, Meyerson M, Lander ES and Getz G: Sensitive detection of somatic point mutations in impure and heterogeneous cancer samples. *Nat Biotechnol* 31: 213-219, 2013.
17. Wang D, Li C, Xu Y, Xing Y, Qu L, Guo Y, Zhang Y, Sun X and Suo J: Clinicopathological characteristics and prognosis of alpha-fetoprotein positive gastric cancer in Chinese patients. *Int J Clin Exp Pathol* 8: 6345-6355, 2015.
18. Lin CY, Yeh HC, Hsu CM, Lin WR and Chiu CT: Clinicopathological features of gastric hepatoid adenocarcinoma. *Biomed J* 38: 65-69, 2015.
19. Xiao C, Wu F, Jiang H, Teng L, Song F, Wang Q and Yang H: Hepatoid adenocarcinoma of the stomach: Nine case reports and treatment outcomes. *Oncol Lett* 10: 1605-1609, 2015.
20. Liu X, Cheng Y, Sheng W, Lu H, Xu Y, Long Z, Zhu H and Wang Y: Clinicopathologic features and prognostic factors in alpha-fetoprotein-producing gastric cancers: Analysis of 104 cases. *J Surg Oncol* 102: 249-255, 2010.
21. Motoyama T, Aizawa K, Watanabe H, Fukase M and Saito K: alpha-Fetoprotein producing gastric carcinomas: A comparative study of three different subtypes. *Acta Pathol Jpn* 43: 654-661, 1993.
22. Chen Y, Qu H, Jian M, Sun G and He Q: High level of serum AFP is an independent negative prognostic factor in gastric cancer. *Int J Biol Markers* 30: e387-e393, 2015.
23. Garber K: From human to mouse and back: 'Tumorgraft' models surge in popularity. *J Natl Cancer Inst* 101: 6-8, 2009.
24. Hwang CI, Boj SF, Clevers H and Tuveson DA: Preclinical models of pancreatic ductal adenocarcinoma. *J Pathol* 238: 197-204, 2016.
25. Kochi M, Fujii M, Kaiga T, Takahashi T, Morishita Y, Kobayashi M, Kasakura Y and Takayama T: FLEP chemotherapy for alpha-fetoprotein-producing gastric cancer. *Oncology* 66: 445-449, 2004.
26. Back SK, Han SW, Oh DY, Im SA, Kim TY and Bang YJ: Clinicopathologic characteristics and treatment outcomes of hepatoid adenocarcinoma of the stomach, a rare but unique subtype of gastric cancer. *BMC Gastroentero* 11: 56, 2011.
27. Giuffr   G, Ieni A, Barresi V, Caruso RA and Tuccari G: HER2 status in unusual histological variants of gastric adenocarcinomas. *J Clin Pathol* 65: 237-241, 2012.
28. Fang Y, Wang L, Li GM, *et al*: Expression of c-Met, VEGF, EGFR and Her-2 in AFP positive gastric cancer. *Chin J Cancer* 26: 662-669, 2016 (In Chinese).
29. Amemiya H, Kono K, Mori Y, Takahashi A, Ichihara F, Iizuka H, Sekikawa T and Matsumoto Y: High frequency of c-Met expression in gastric cancers producing alpha-fetoprotein. *Oncology* 59: 145-151, 2000.
30. Qin S, Ji J, Xu RH, Wang W, Tang Y, Bi F, Li J, Wang K, Xu JM, Fan Q, *et al*: Treatment patterns and outcomes in chinese patients with gastric cancer by HER2 status: A noninterventional registry study (EVIDENCE). *Oncologist* 26: e1567-e1580, 2021.
31. Chung HC, Bang YJ, S Fuchs C, Qin SK, Satoh T, Shitara K, Tabernero J, Van Cutsem E, Alsina M, Cao ZA, *et al*: First-line pembrolizumab/placebo plus trastuzumab and chemotherapy in HER2-positive advanced gastric cancer: KEYNOTE-811. *Future Oncol* 17: 491-501, 2021.
32. Russell R, Perkhof L, Liebau S, Lin Q, Lechel A, Feld FM, Hessmann E, Gaedcke J, G  thle M, Zenke M, *et al*: Loss of ATM accelerates pancreatic cancer formation and epithelial-mesenchymal transition. *Nat Commun* 6: 7677, 2015.
33. Farmer H, McCabe N, Lord CJ, Tutt AN, Johnson DA, Richardson TB, Santarosa M, Dillon KJ, Hickson I, Knights C, *et al*: Targeting the DNA repair defect in BRCA mutant cells as a therapeutic strategy. *Nature* 434: 917-921, 2005.



This work is licensed under a Creative Commons Attribution-NonCommercial-NoDerivatives 4.0 International (CC BY-NC-ND 4.0) License.